Gnielinski's correlation and a modern temperature-oscillation method for measuring heat transfer coefficients

Martin Dostál[1,*], *Karel* Petera[1], and *Stanislav* Solnař[1]

[1]Czech Technical University in Prague, Faculty of Mechanical Engineering, Department of Process Engineering, Technická 4, 166 07 Prague, Czech Republic

Abstract. The heat transfer coefficient is one of the most important parameters in the design of apparatuses in which convective heat transport takes place. Classical direct methods based on determining basic thermal quantities can be used for measuring heat transfer coefficients. Another option is to measure concentrations, electric current or other quantities that can be transformed to thermal quantities using the analogy between heat and mass transport. The temperature-oscillation method is less frequently used, although the theoretical basis of the method dates back to 1997, and although the method has the major advantage that the heat transfer coefficients can be measured without making any contact with the heat transfer surface. In the temperature-oscillation method, the heat transfer surface is exposed to an oscillating heat flux, and the temperature response on this surface can be measured by a contactless method (e.g. infra-red thermography). The heat transfer coefficients can be determined on the basis of mathematical relations between the oscillating heat flux and the temperature response. However, the method depends on an appropriate method for processing the measured data when it is necessary to correct some conditions that are not included in the mathematical model. This paper evaluates the impact of processing the experimental data on the resulting heat transfer coefficients in one of the basic geometrical configurations – the flow of a liquid in a pipe with a circular cross section. In this paper, we present the results of a comparison of real experiments based on the temperature oscillation method and numerical modeling of the heat transfer in this geometry, using the ANSYS CFD commercial system.

1 Introduction

Experimental methods based on temperature oscillations have been known and used for a long time. They mainly use knowledge of an analytical solution of the temperature field in a solid body that is exposed to a periodic (oscillating) heat flux. For example, the excellent book by Carslaw and Jaeger [1] presented an analytical solution of heat conduction in infinite and semi-infinite bodies, walls, cylinders, spheres, etc., for step changes or oscillating in temperature. Carslaw and Jaeger mentioned the use of these non-stationary solutions for determining the thermophysical properties of materials. Hausen [2] also provided an analysis of determining the heat transmission coefficient (the overall heat transfer coefficient, which describes the transfer of heat through a wall) based on the known temperature field in a regenerator.

Roetzel [3] described an experimental technique and an evaluation of local heat transfer coefficients on the surface of a pipe or other channels based on measuring the wall temperature oscillations caused by a periodic change in the temperature of the liquid flowing in the channel. Good agreement of the experimental results compared with the Hausen correlation were mentioned. Roetzel et al. [4] described a similar technique for measuring the heat transfer coefficient in a plate heat exchanger. The mathematical model of the heat transfer presented in paper [4] included the axial dispersion coefficient, which can also be determined. Roetzel and Luo [5] further improved this technique. They used a computer-controlled electric heating body to generate sine temperature oscillations at the inlet of the heat exchanger. Leblay et al. [6] used the temperature oscillation method to measure the heat transfer in a circular tube and in a multiport-flat tube at Reynolds numbers between 800 and 14000. The temperature oscillations were invoked by Joule's heat, and the temperature response was measured by infrared thermography.

Roetzel et al. [7] described a new experimental technique based on periodic heating of the heat transfer surface by a laser. They measured the heat transfer coefficients on the inner side of an agitated vessel. The temperature response on the outer side of the heat transfer surface was determined by a contactless method. Smaller heat transfer coefficients than the standard correlations were obtained, and better agreement was observed at higher Reynolds numbers (about 15000). They measured approximately 50% values at lower Reynolds numbers (2000).

In 1997, Wandelt and Roetzel [8] published the solution of the temperature field in an infinite plate with oscillating heat flux irradiating one side. The resulting harmonic oscillations in the temperature field are influenced

*e-mail: martin.dostal@fs.cvut.cz

by the heat transfer coefficients on both sides of the plate, and they can be used in determining these coefficients.

Freund and Kabelac [9] tested the method described in [8], known also as Lock-In-Thermography, on a semi-infinite body and on the inlet section of a (copper) pipe, where hydrodynamic and thermal boundary layers were developing. They used a laser diode array with a wave length of 785 nm and power of 15 W to generate temperature oscillations. The temperature responses at the surface were monitored by an infra-red camera with a frame rate of 30 fps. They obtained a 0.1 % deviation from the theoretical phase shift for frequencies of 0.1 Hz, 0.5 Hz, and 0.05 Hz. A laser spot 30 mm in diameter and with sine-modulated intensity with a frequency of 0.1 Hz was used for measuring the heat transfer in the pipe, and the preliminary results agreed with standard engineering correlations. Freund [10] focused on the temperature oscillation method, using contactless measurements of the temperature response (Temperature Oscillation Infra-Red Thermography) and algorithms for processing the measured data. Freund and Kabelac [11] applied the temperature oscillation method for measuring the heat transfer on the plates of a plate heat exchanger. The oscillating heat flux was generated by an array of halogen spotlights with a total of more than 3 kW electric power. The turbulent flow between the plates of the heat exchanger was modeled using the ANSYS® CFX® commercial CFD software package. The Shear-Stress-Transport (SST) and Reynolds-Stress Model (RSM) turbulence models were used. A comparison between the experiments and the numerical simulations showed that the mean heat transfer coefficients based on the SST model are 33 % lower than the experimental values. In the case of RSM, they are 25 % lower.

The works cited here show that the biggest advantage of this method is the contactless determination of the surface temperatures (Temperature Oscillation Infra-Red Thermography = TOIRT). However, few papers have been published on this topic in recent years, although heat transfer coefficients are very important in the design of many industrial apparatuses. Possible reasons may be that experimental investigations of heat transfer have been replaced by numerical simulations, which are, in many cases, cheaper than building an experimental device and measuring the results in the laboratory or on real equipment. However, experimental data still have an important role in verifying the results of numerical models.

Another reason for the less frequent application of the TOIRT method could lie in the contactless measurements of the temperatures. Precise infra-red cameras are nowadays available, but they may be too expensive for some experimental groups. Widely-available cameras, mostly based on the bolometric method, have relatively large thermal sensitivity, but they still have substantial uncertainty when measuring absolute temperature values. For example, the thermal sensitivity (NETD) of our thermoImager TIM 160 camera is 80 mK, but the resolution is 0.1 °C, and the accuracy is ±2 °C or ±2 %, whichever is greater [https://www.micro-epsilon.com]. The Gobi-640-GigE camera has thermal sensitivity of 55 mK at 30 °C [http://www.xenics.com]. The FLIR A325sc infra-red camera has thermal sensitivity lower than 50 mK and accuracy ±2 °C or ±2 % [https://www.termokamery-flir.cz].

Taking into account that oscillations with amplitudes smaller than 1 °C can be measured with the TOIRT method, the accuracy of the temperature measurements might be limiting. An advantage of TOIRT is that it is not necessary to know the absolute value of the temperature, it is sufficient to determine the shape of its response, the phase shift, which, however, can be influenced by the integration type (rolling shutter, snapshot) and by the integration time. The integration times are of the order of μs up to tens of ms. The resolution of the camera, and also the specific lens, affects the size of the monitored region and the corresponding surface on which the heat transfer coefficients can be investigated.

Our tests of the TOIRT method investigated the flow of a Newtonian liquid in a pipe with a circular cross section. In the fully developed turbulent flow regime, Gnielinski's correlation [12] describes the mean Nusselt number ($\mathrm{Nu} = \alpha d/\lambda_\mathrm{f}$) in a straight pipe for $\mathrm{Re} \geq 10^4$ ($10^6 \geq \mathrm{Re} \geq 10^4$, $0.1 \leq \mathrm{Pr} \leq 1000$)

$$\mathrm{Nu_m} = \frac{(\xi/8)\ \mathrm{Re\,Pr}}{1 + 12.7\sqrt{\xi/8}\left(\mathrm{Pr}^{2/3} - 1\right)}\left[1 + \left(\frac{d}{L}\right)^{2/3}\right], \quad (1)$$

where ξ is the Darcy-Weisbach friction coefficient, which can be expressed, as recommended by [12], using the Konakov relation for smooth pipes

$$\xi = (1.8 \log \mathrm{Re} - 1.5)^{-2}\ . \quad (2)$$

The last term in (1) represents the Hausen correction factor, which takes into account the substantial increase in heat transfer for short pipes. This correction factor is for a pipe with $d = L$ equal to 2. The correction factor decreases to 1.2 for the case $d = 2L$, to 1.025 for $d = 5L$, to 1.005 for $d = 10L$, and it approaches a value of 1 with increasing pipe length. A local increase in the heat transfer coefficient is still present at the beginning of a longer pipe, but it has a small impact on the average value along its length. If we measure local values of the heat transfer coefficients, we can compare the results with the derivative of Eq. (1), as stated by [12].

$$\mathrm{Nu_x} = \frac{(\xi/8)\ \mathrm{Re\,Pr}}{1 + 12.7\sqrt{\xi/8}\left(\mathrm{Pr}^{2/3} - 1\right)}\left[1 + \frac{1}{3}\left(\frac{d}{x}\right)^{2/3}\right] \quad (3)$$

In the case of laminar flow in a pipe with a circular cross section with a constant wall temperature, the Hausen correlation [2] describes the mean value of the Nusselt number

$$\mathrm{Nu_m} = 3.66 + \frac{0.0668\,\mathrm{Gz}}{1 + 0.045\,\mathrm{Gz}^{2/3}}\ ,\ \mathrm{Gz} = \mathrm{Re\,Pr}\,d/L\,. \quad (4)$$

This relation meets the limits for long pipes and also for short pipes. In the case of short pipes, Léveque derived [12],

$$\mathrm{Nu_m} = 1.615\,\mathrm{Gz}^{1/3} \quad (5)$$

which can be transformed to

$$\mathrm{Nu_x} = 1.077\,\mathrm{Gz_x}^{1/3}\ ,\ \mathrm{Gz_x} = \mathrm{Re\,Pr}\,d/x \quad (6)$$

Table 1. Thermophysical properties of widely-used engineering materials at a temperature of 20 °C, see [13] and [https://www.foamglas.com].

Material	λ	c_p	ϱ
	$\mathrm{W\,m^{-1}\,K^{-1}}$	$\mathrm{J\,kg^{-1}\,K^{-1}}$	$\mathrm{kg\,m^{-3}}$
stainless steel	15.2	501	7900
carbon steel	49.8	465	7840
aluminium	236	902	2710
copper	398	386	8930
FOAMGLASS ®W+F	0.038	1000	100
glass	0.76	840	2710

for local values of the Nusselt numbers at distance x from the beginning of the pipe.

In our experimental work, we had to deal with many problems connected with the application of the TOIRT method. In the following text, we therefore analyze the impact of some parameters on the accuracy of this method.

2 TOIRT basis

As has been mentioned above, Wandelt and Roetzel [8] published an analytical steady periodic solution of the temperature field on the surfaces of an infinite plate with width δ (Figure 7, on the right) described by the one-dimensional Fourier equation

$$\frac{\partial T}{\partial t} = a\frac{\partial^2 T}{\partial x^2}\,. \tag{7}$$

The plate has zero initial temperature ($T_0 = 0$). It is surrounded by a fluid at zero temperature ($T_\mathrm{f} = 0$). Boundary conditions of the third kind are described by the heat transfer coefficients on both sides of the plate (α a α_δ), and a boundary condition of the second kind is represented by the heat flux on one side of the plate ($q|_{x=\delta} = \hat{q}\sin\omega t$), which oscillates around a mean value of zero

$$-\lambda\left.\frac{\partial T}{\partial x}\right|_{x=0} = -\alpha\,T|_{x=0}\;,\; -\lambda\left.\frac{\partial T}{\partial x}\right|_{x=\delta} = -\hat{q}\sin\omega t + \alpha_\delta\,T|_{x=\delta}\;. \tag{8}$$

The steady periodic temperature solution can be expressed in a general form as a function of amplitude A and phase shift φ

$$T(x,t) = A(x)\sin\left[\omega t - \varphi(x)\right]\,. \tag{9}$$

Wandelt and Roetzel [8] presented analytical formulas for A and φ, which depend on geometric parameters, thermophysical properties and the heat transfer coefficients α and α_δ on the two sides.

We will now illustrate here the graphical solution of Wandelt and Roetzel for some parameters that can be met in practical situations. The width of the heat exchange surface δ is usually within the order of millimeters, and we will therefore use 0.5, 1, 1.5 and possibly 2 mm. Table 1 describes thermophysical parameters of widely-used engineering materials (stainless steel, carbon steel, aluminium, and copper). All these materials can be met in the design of real apparatuses, but we will place the emphasis here on stainless steel, because it is the material that we used in our experimental work.

Figure 1 describes the dependency of the heat transfer coefficient α on the phase shift $\varphi|_{x=\delta}$ between the heat flux and the surface temperature response for a plate 1.5 mm in width made of stainless steel, for three different frequencies of the oscillating heat flux. It can be clearly seen here that the common frequency 0.1 Hz covers heat transfer coefficients values from hundreds to thousands of $\mathrm{W\,m^{-2}\,K^{-1}}$. However, this dependency is quite steep for large heat transfer coefficients values, so a small inaccuracy in the phase shift has a big impact on the evaluated coefficients. The relative inaccuracy of the heat transfer coefficient is depicted by dotted lines. These lines represent the relative change in the heat transfer coefficient with respect to the change in the phase shift. The relative inaccuracy can be expressed as derivative $1/\alpha \cdot \mathrm{d}\alpha/\mathrm{d}\varphi$ (displayed as a percentage, i.e., it has been multiplied by 100 in the Figure). It is clear that the smallest errors in the heat transfer coefficients can be achieved when the phase shift is around 45°. In this region, a change of ±1° in the phase shift causes a relative error of approximately ±5 %. Similar relationships can be illustrated for other considered plate widths, 0.5 and 1.0 mm.

Figures 2 illustrate the Wandelt-Roetzel solution for various widths (left) and materials (right) of the plate. It is interesting that the plate material (i.e. the heat transfer surface) does not have a large impact on the shape and the position of the dependency. We can therefore state that the plate can be made from stainless steel, and also from copper (of course, taking other parameters into account, e.g. the plate width of 1 mm). However, the width of the plate has a greater influence, see Figure 2, on the left. If we want to be in a region with reasonable accuracy, we should therefore have in mind that a thicker plate substantially reduces the region with corresponding phase shifts. Interestingly, the relative error of the heat transfer coefficient is same as for thinner plates.

The graphical dependencies presented here clearly show that the phase shift should lie within 20 – 70° for

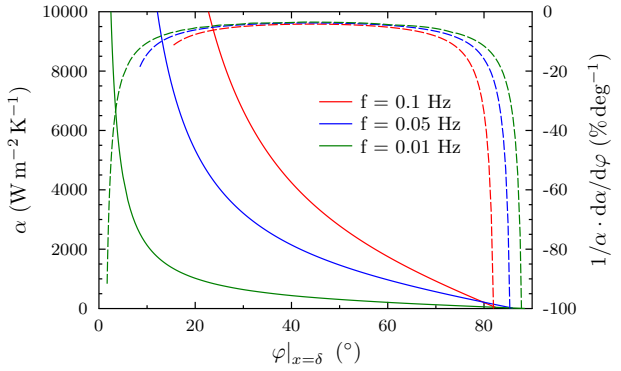

Fig. 1. The dependency of heat transfer coefficient α on phase shift $\varphi|_{x=\delta}$ for different frequencies of the oscillating heat flux (full lines). The dotted lines represent the relative sensitivity of the heat transfer coefficient with respect to the phase shift, which is the derivative $1/\alpha \cdot \mathrm{d}\alpha/\mathrm{d}\varphi$ (see the right axis). The plate width is 1.5 mm, stainless steel, see properties in Table 1. The heat transfer on the irradiated side is 3 $\mathrm{W\,m^{-2}\,K^{-1}}$.

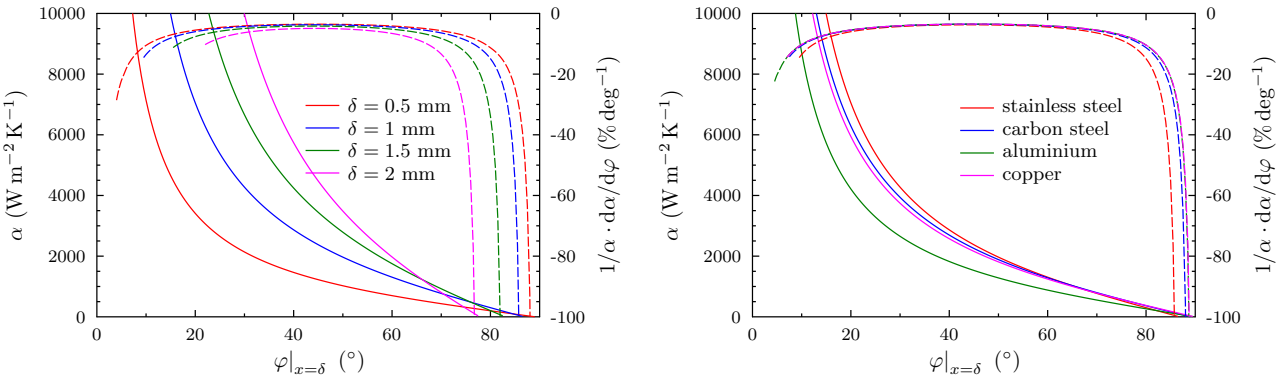

Fig. 2. The dependency of heat transfer coefficient α on phase shift $\varphi|_{x=\delta}$ for different wall widths (left) and for different materials (right). The dotted lines represent the relative sensitivity of the heat transfer coefficient with respect to the phase shift, which is the derivative $1/\alpha \cdot \mathrm{d}\alpha/\mathrm{d}\varphi$ (see the right axis). The dependency is illustrated for 0.1 Hz frequency of the oscillating heat flux. The wall material is stainless steel, see properties in Table 1. The heat transfer on the irradiated side is 3 W m^{-2} K^{-1}.

the frequency of the oscillating heat flux 0.1 Hz and for plate width up to 1.5 mm. In this case, the relative error is within an acceptable range $\mp 5 - 10$ % for inaccuracy $\pm 1°$ of the phase shift.

The figures illustrate Wandelt and Roetzel's solution in graphical form. In cases where we are able to measure the surface temperature on the side irradiated by the sine-oscillating heat flux and where we can determine the phase shift, we can read the corresponding heat transfer coefficient value. The basis of this method appears simple, but it is based on assumptions that cannot be precisely met in a real experiment:

- Zero ambient fluid temperature conditions and zero initial temperature condition, or, in other words, conditions with the same initial temperature of the plate and of the surrounding fluid.
- A steady-state periodic regime that does not take into account the transitional change at the beginning of the temperature oscillations (at the beginning of the measurements).
- Temperature oscillations with a zero mean value, i.e. they are positive (heating) in the first part of the sine period and negative (cooling) in the second part. These oscillations around a zero value cannot be achieved in a real experiment. Due to the continuous temperature increase of the wall irradiated by the heat flux, the measured temperature response will oscillate around a non-oscillating component which changes with time.

3 Transitional change and dynamic equilibrium

To better analyse the assumptions of the Wandelt-Roetzel solution and their impact on the evaluated heat transfer coefficient, we implemented a numerical solution of the heat conduction equation (7), along with the initial and boundary conditions (8), using the **pdepe** function in MATLAB® software. Some details of the solution can be found in the Appendix. Only graphical results will be presented and discussed in this section.

Figure 3 (left) compares the numerical and Wandelt-Roetzel solutions for the case with zero mean value of the heat flux. It is clear that the transitional change at the beginning disappears approximately after the second period, and the numerical solution then copies the analytical solution of Wandelt and Roetzel. This figure represents the case of heat transfer coefficient $\alpha = 1000$ W m^{-2} K^{-1}, and the impact of the transient change at the beginning is reduced with higher heat transfer coefficients. The impact of the transitional change is illustrated here by the green dashed line, as the absolute difference between the numerical solution and the analytical solution. It is interesting that this difference is very similar to the exponential function, which represents the response of the first-order system to the step change of the boundary condition, which is characterized by some time constant (for corresponding parameters, of course, it is not correct in general).

For technical reasons, it is not possible to have the heat flux oscillating around a mean value of zero. In practice, the plate is heated by an oscillating heat flux with non-zero mean value $\bar{q}$, and the oscillations of the temperature response are also around a non-zero mean value, and, in addition, that non-zero temperature mean value is time-dependent. Figure 3 (right) presents the solution of the problem with a non-zero mean value of the heat flux. In this case, the mean value is $\bar{q} = 2000$ W m^{-2} and the amplitude is $\hat{q} = 1000$ W m^{-2}. A transient change can be observed at the beginning. It briefly approaches the steady harmonic oscillations of the temperature corresponding to the Wandelt-Roetzel solution, but now around non-zero value $T|_{x=\delta,\mathrm{eq}}$. The steady mean temperature is due to the stationary solution of the heat conduction in the plate (7) with boundary conditions (8). In this case, for the boundary condition on the side of the heat flux, which is in the position $x = \delta$, the harmonic function $\hat{q} \sin \omega t$, is replaced by constant value $\bar{q}$. The solution of this equation for the steady-state case, i.e. $\partial T/\partial t = 0$, and zero surrounding

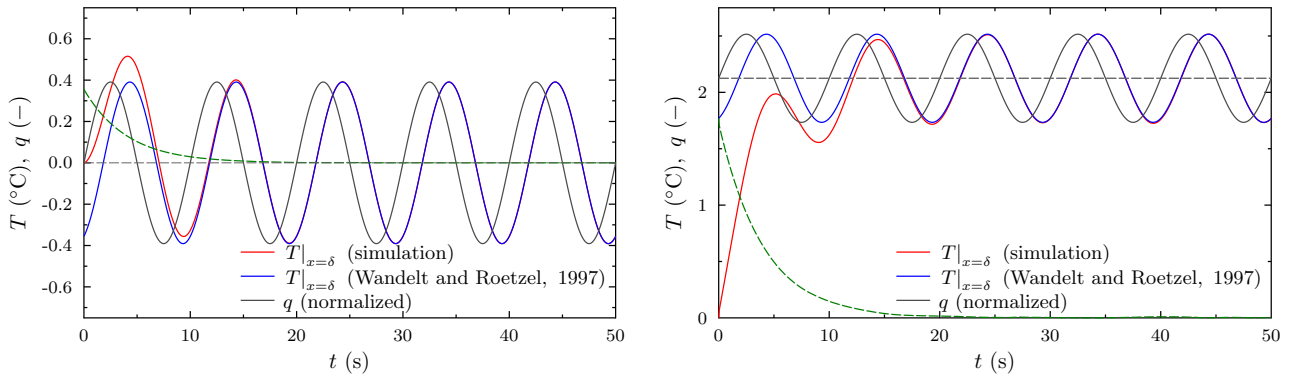

Fig. 3. Temperature response on the surface of the plate (red line) to the harmonic oscillating heat flux (black line), and a comparison with oscillations corresponding to the Wandelt-Roetzel solution (blue line, and the green dashed line represents the difference between them) for heat transfer coefficient 1000 W m^{-2} K^{-1}. The plate 1 mm in width is made from stainless steel. Heat transfer coefficient α_δ is 3 W m^{-2} K^{-1}. The amplitude of the heat flux oscillations is 1000 W m^{-2}, with a zero mean value (left), in comparison with a dependency with a mean value of 2000 W m^{-2} (right).

temperature $T_\mathrm{f} = 0$ is

$$T|_{x=\delta,\,\mathrm{eq}} = \bar{q}\frac{\delta + \dfrac{\lambda}{\alpha}}{\alpha_\delta\delta + \dfrac{\lambda}{\alpha} + \lambda}\,. \tag{10}$$

Similarly as with the zero mean value of the heat flux, the length of the transitional initial period decreases with increasing heat transfer coefficients. For a 1 mm plate, it is relatively short. To illustrate its impact, see Figure 4 corresponding to the solution with a plate width of 10 mm. It is clear that the transitional period is very long and we do not approach constant mean temperature even after 10 oscillations.

Making measurements with plates of greater width means that we would have to wait a long time to reach the steady-state mean value, especially for smaller heat transfer intensities. In practise, we can encounter this situation

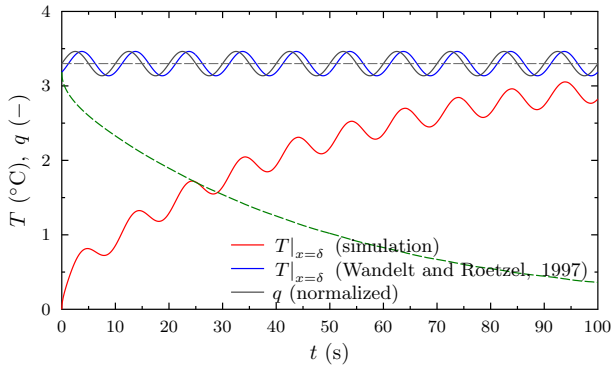

Fig. 4. Temperature response on the surface of the plate (red line) to the harmonic oscillating heat flux (black line), and a comparison with oscillations corresponding to the Wandelt-Roetzel solution (blue line, and the green dashed line represents the difference between them) for heat transfer coefficient 1000 W m^{-2} K^{-1}. The plate 10 mm in width is made from stainless steel. Heat transfer coefficient α_δ is 3 W m^{-2} K^{-1}. The amplitude of the heat flux oscillations is 1000 W m^{-2}, with a mean value of 2000 W m^{-2}.

even with a plate width of 1 or 1.5 mm. The question is whether we can use the measured response even in cases when we do not reach these steady state oscillations.

Another question is whether we could make an estimate of the length of this transitional region. As has already been mentioned above, the exponential character of the time dependency would correspond to the response of a 1st order system induced by a unit step change, which is the response of the system characterized by the heat capacity of the plate. Assuming the simplest case, with a constant temperature inside the plate, we could determine the time constant of the transition process as

$$\tau = \frac{M\,c_p}{(\alpha+\alpha_\delta)\,S} = \frac{S\,\delta\varrho c_p}{(\alpha+\alpha_\delta)\,S} = \frac{\delta\varrho c_p}{(\alpha+\alpha_\delta)} = \frac{\delta\lambda}{a\,(\alpha+\alpha_\delta)}\,, \tag{11}$$

where M is the mass of a plate of width δ, surface S and density ϱ. Assuming that the whole mass of the plate is concentrated into a single mass point of constant temperature, i.e. for the Biot number $\mathrm{Bi} = \alpha\delta/\lambda \ll 1$,we could simply express the temperature oscillations around the temperature given by the transition process as

$$T|_{x=\delta} = T|_{x=\delta,\,\mathrm{eq}} - \left(T|_{x=\delta,\,\mathrm{eq}} - A|_{x=\delta}\sin\varphi|_{x=\delta}\right)\mathrm{e}^{-t/\tau} + \\ + A|_{x=\delta}\sin\left(\omega t - \varphi|_{x=\delta}\right)\,, \tag{12}$$

where the amplitude and the phase shift of the harmonic oscillations are given by relation (9), and the steady-state temperature and the time constant are given by (10, 11).

4 Eliminating a non-oscillating component

The crucial step in the TOIRT method, which affects its accuracy, is to eliminate the non-oscillating component of the measured temperature response. The aim is for the resulting signal to oscillate around the zero mean value after this elimination, as depicted in Figure 3 (left).

One option could lie in a theoretical solution of the non-oscillating component. In the simplest case, it can be

replaced by an exponential function (especially when the heat transfer surface is made of a material with high heat conductivity – e.g. aluminum or copper). In a more general case, when this kind of simplification cannot be used, we can use an empirical approach and find a suitable algorithm, and then verify it. Solnař [14] describes an algorithm based on several steps: (a) the measured temperature signal is divided into whole periods, (b) the mean temperature is calculated in each period, (c) this temperature moves to the beginning of the period and creates a piecewise linear correction function, (d) this correction function is subtracted from the measured signal. The whole procedure is repeated several times, until the correction function is smaller than a chosen number.

Figure 5 at the top illustrates a practical example of the time dependency of the surface temperature when measuring heat transfer coefficients in a pipe (see the last section of this paper for specific parameters). The bottom part of this figure displays the results of this procedure (red line with black dots).

These transformed data can then be used to find the corresponding phase shift. This can be determined by

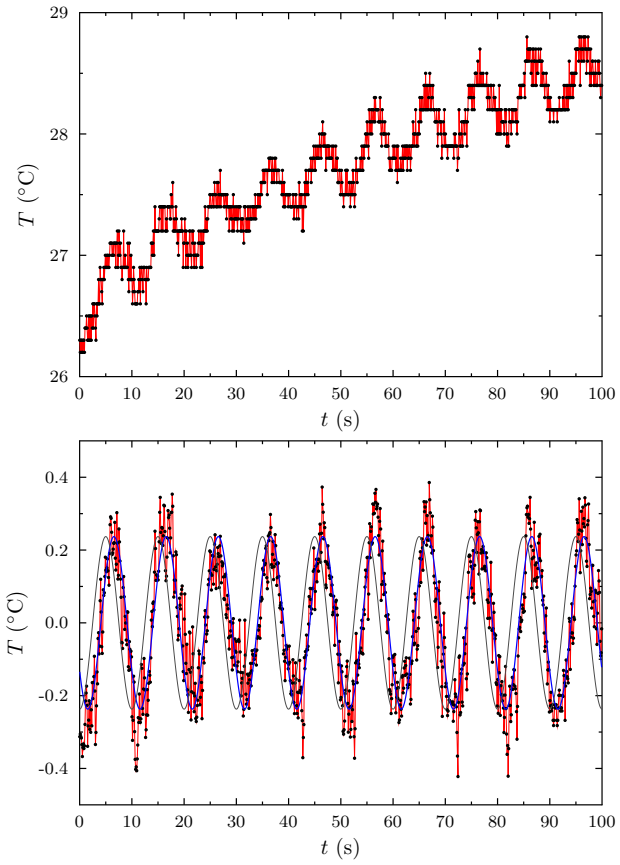

Fig. 5. (top) Measured temperature response for one point on the surface of the pipe. (bottom) The same data after the transformation procedure to eliminate the non-oscillating mean component of the signal (black points). The blue line represents the result of nonlinear regression using sine function, see Eq. (9), which should correspond to the oscillating heat flux irradiating the heat transfer surface (see the gray line, which here offers just an approximate illustration of the temperature response phase shift).

the Fourier transform, or by using the nonlinear regression procedure (the **nlinreg** function in MATLAB®). It is based on minimizing the sum of squares, in our case

$$\sum_{i=1}^{N} \left[T_i - A \sin\left(\omega t_i + \varphi\right)\right]^2 = \min , \tag{13}$$

where A and φ are the amplitude and the phase shift of the sine temperature response, N is the number of experimental points, i.e. couples of temperatures T_i and times t_i, and ω is the angular frequency of the oscillating heat flux. We could evaluate the phase shift 303.678°, or −56.322°, for the experimental data in Figure 5.

It is obvious that the algorithm for eliminating the non-oscillating component of the measured temperature response can have a huge impact on the evaluated experimental results. Let us test its influence on model data prepared with a function of given parameters, so that we can make an estimate of the inaccuracies when using this procedure. The model data were based on the following function

$$T = \underbrace{a + b\left(1 - \mathrm{e}^{-t/\tau}\right)}_{\text{steady part}} + \underbrace{A \sin\left(\omega t + \varphi\right)}_{\text{harmonic part}} + \underbrace{\mathrm{randn}\left(\sigma\right)}_{\text{noise}} , \tag{14}$$

where a and b are additional parameters affecting the shape of the signal, and σ is the standard deviation of random data with a normal distribution around a mean value of zero.

The algorithm was tested for a signal with frequency 0.1 Hz, sampled frequency 10 Hz, and various shapes (a pure sine signal, a sine signal superposed on an exponential function with a shift, a signal with superposed noise, and a quantum signal with a specific minimal temperature resolution size, for example 0.1 °C).

Table 2 shows the results of eliminating the non-oscillating component in the case of a model harmonic signal with two amplitudes. The algorithm that is used clearly provides adequate results for the phase shift in the whole range – the maximum absolute deviation is 0.31°. These deviations decrease with increasing amplitude of the oscillations.

In practice, the measured signal is noisy and, according to the infra-red camera, the measured temperatures are resolved with quantum steps of 0.1 °C. In this case, the deviations are substantially larger, see Table 3. The tables show the results for only one run and one shape. When processing many randomly generated noisy data, we get a maximum deviation of ±2.45°, and for the case of a quantum signal a maximum deviation of ±2.88°.

5 Phase shift in real measurements

In the previous section, algorithms for evaluating the heat transfer coefficient with the TOIRT method were described, under the assumption that only the temperature response suffers from measurement inaccuracies, but that the heat flux and time are measured and set precisely. This is quite important, because the resulting phase of the temperature response is used in the evaluation. In reality, however, the situation is different.

Table 2. Deviations in processing a harmonic signal with frequency 0.1 Hz ($\omega = 2\pi\,0.1\ \mathrm{s}^{-1}$) superposed on the exponential function for amplitudes $A = 0.5$ °C and 1 °C. The sampled frequency is 10 Hz, and the signal length is 100 s.

$$T = 25 + 4\left(1 - \mathrm{e}^{-t/100}\right) + A\sin\left(\omega\, t + \varphi_{\mathrm{set}}\right)$$

	$A = 0.5$ °C		$A = 1$ °C	
φ_{set} (°)	φ (°)	$\Delta\varphi$ (°)	φ (°)	$\Delta\varphi$ (°)
0	-0.15	-0.15	-0.08	-0.08
5	4.88	-0.12	4.94	-0.06
10	9.90	-0.10	9.95	-0.05
15	14.93	-0.07	14.97	-0.03
20	19.96	-0.04	19.98	-0.02
25	24.99	-0.01	25.00	-0.00
30	30.02	0.02	30.01	0.01
35	35.05	0.05	35.03	0.03
40	40.08	0.08	40.04	0.04
45	45.11	0.11	45.06	0.06
50	50.14	0.14	50.07	0.07
55	55.17	0.17	55.08	0.08
60	60.19	0.19	60.10	0.10
65	65.22	0.22	65.11	0.11
70	70.24	0.24	70.12	0.12
75	75.26	0.26	75.13	0.13
80	80.28	0.28	80.14	0.14
85	85.30	0.30	85.15	0.15
90	90.31	0.31	90.16	0.16

Table 3. Deviations in processing a harmonic signal with frequency 0.1 Hz ($\omega = 2\pi\,0.1\ \mathrm{s}^{-1}$) superposed on an exponential function with standard deviation of 0.2 °C for amplitude $A = 0.5$ °C. Sample frequency 10 Hz, signal length 100 s. The results for a non-rounded signal are shown in the columns on the left. The results for a signal with quantum resolution of 0.1 °C are shown in the columns on the right.

$$T = 25 + 3\left(1 - \mathrm{e}^{-t/100}\right) + A\sin\left(\omega\, t + \varphi_{\mathrm{set}}\right) + \mathrm{randn}\,(0.2)$$

	noise		noise & quant	
φ_{set} (°)	φ (°)	$\Delta\varphi$ (°)	φ (°)	$\Delta\varphi$ (°)
0	1.21	1.21	1.12	1.12
5	6.20	1.20	6.23	1.23
10	11.18	1.18	11.20	1.20
15	16.16	1.16	16.30	1.30
20	21.12	1.12	21.04	1.04
25	26.08	1.08	26.10	1.10
30	31.03	1.03	31.10	1.10
35	35.97	0.97	36.04	1.04
40	40.91	0.91	41.08	1.08
45	45.83	0.83	45.80	0.80
50	50.76	0.76	50.76	0.76
55	55.67	0.67	55.94	0.94
60	60.58	0.58	60.32	0.32
65	65.49	0.49	65.49	0.49
70	70.39	0.39	70.54	0.54
75	75.29	0.29	75.28	0.28
80	80.19	0.19	80.28	0.28
85	85.09	0.09	84.88	-0.12
90	89.99	-0.01	90.12	0.12

The oscillating heat flux is generated by a set of one or more halogen lamps, each with power of 500 W in our experiments. The power supply of direct voltage 0 – 230 V with a maximum of 1600 W [https://www.bke.cz/cs/produkty/js-2k0-2k0nv] is controlled by the BK Precision 4052 precise two-channel signal generator [http://www.bkprecision.com/products/signal-generators/4052-5-mhz-dual-channel-function-arbitrary-waveform-generator.html]. One channel of this generator creates the sine signal that controls the power supply of the halogen lamps. The second channel generates trigger square pulses for the thermoIMAGER TIM 160 infra-red camera [https://www.micro-epsilon.com/temperature-sensors/thermoIMAGER/]. The timings of the trigger pulses and the generated signal for the power supply are depicted in Figure 6. It is clear that the first trigger pulse for the camera measuring the temperature is delayed behind the signal controlling the heat flux. This delay does not cause any problem in the evaluation, because it is precisely defined, and can be taken into account. The problem lies especially in the dynamic characteristics of the power supply and the halogen lamps, which generate the heat flux. Assuming that the system, the power supply – the halogen lamps, behaves as a system of the first order, we can describe it by time constant τ (which is of course not same as the time constant of the temperature response in the previous section). In the case of harmonic oscillations, this time constant will represent the delay of the generated heat flux with respect to the control signal in the generator, which ensured the synchronization of the measurement. This time constant, or its corresponding phase shift, must be used to decrease the evaluated phase shift from the experimental data.

The most practical way to determine the time constant would be by measuring the heat transfer coefficient on a geometry where it is precisely known. Using the methods mentioned above, we could determine this additional compensation of the phase shift in such a way that the determined value would be equal to the known value. The problem is the precision of the known value of the heat transfer coefficient. Most verified correlations (a semi-infinite

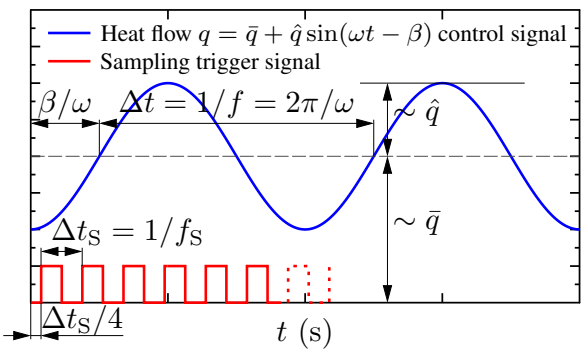

Fig. 6. Illustration of the time dependencies of the signal controlling the generated heat flux and the sampling signal for measuring the temperature.

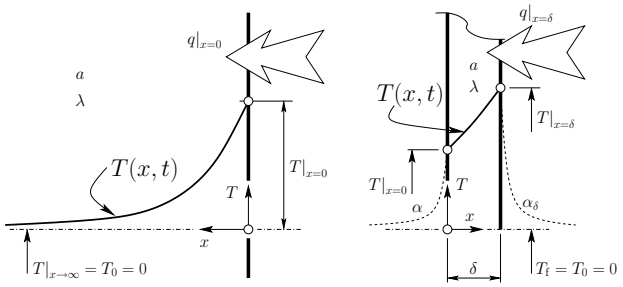

Fig. 7. A semi-infinite body as a calibration tool of the TOIRT method (left), and the heat transfer surface of an infinite plate (right). The boundary condition of the harmonic oscillating heat flux $q|_{x=\delta} = \bar{q} + \hat{q}\sin(\omega t - \beta)$ is applied to the heat transfer surface (wall) with the TOIRT method (the Wandelt-Roetzel solution assumes $\bar{q} = 0$ and $\beta = 0$).

body, a plate of finite width, an impinging jet, the flow in a pipe of circular cross section) already have some non-zero deviation from the "theoretical" value, although they have been in use for many years.

Another possible approach would be to make measurements on a geometry where the value of the heat transfer coefficient has no impact or a very small impact on the results. A semi-infinite body is one of the options, see Figure 7 (left).

Carslaw and Jaeger [1] describe the solution of the temperature field in a semi-infinite body for the case of harmonic oscillations of the surface temperature (page 64), which is the boundary condition $T|_{x=0} = A\cos\omega t$ (including the phase shift β which is not mentioned here) and for the zero initial temperature $T_0 = 0$.

$$T(x,t) = A\mathrm{e}^{-\sqrt{\frac{\omega}{2a}}x}\cos\left(\omega t - \sqrt{\frac{\omega}{2a}}x\right) + \\ - \frac{2A}{\sqrt{\pi}}\int_0^{x/\sqrt{4at}}\cos\left\{\omega\left(t - \frac{x^2}{4a\mu^2}\right)\right\}e^{-\mu}\mathrm{d}\mu\,, \quad (15)$$

The solution consists of the steady periodic part (first term/row) and the transient part (second term/row). The transient part expresses the disturbance caused by starting the oscillations, which disappears with increasing time. The term $x\sqrt{\omega/2a}$ represents the dimensionless coordinate here, and we can define the characteristic length using the penetration depth $\delta \sim \sqrt{a/\omega}$.

Expressing the heat flux on the surface of the semi-infinite body using the Fourier law and only the steady-periodic part, we get

$$q|_{x=0} = -\lambda\left.\frac{\partial T}{\partial x}\right|_{x=0} = -\lambda\cdot A\sqrt{\frac{\omega}{2a}}\mathrm{e}^{-\sqrt{\frac{\omega}{2a}}x}\cdot \\ \cdot\sin\left(\omega t - \sqrt{\frac{\omega}{2a}}x\right) - \cos\left(\omega t - \sqrt{\frac{\omega}{2a}}x\right)\Big|_{x=0} = \\ = \underbrace{\lambda A\sqrt{\frac{\omega}{a}}}_{\hat{q}}\cos\left(\omega t + \frac{\pi}{4}\right). \quad (16)$$

It can be seen here that the heat flux on the surface of the semi-infinite body is phase-shifted by $\pi/4$, and the leading factor of the goniometric function represents the amplitude. Assuming periodic heat oscillations on the surface, which is the boundary condition $q|_{x=0} = \hat{q}\cos\omega t$, the corresponding temperature response on the surface of the semi-infinite body (steady periodic part) can be described as

$$T|_{x=0} = \frac{\hat{q}}{\lambda\sqrt{\frac{\omega}{a}}}\cos\left(\omega t - \frac{\pi}{4}\right). \quad (17)$$

We can see here that the semi-infinite body could be advantageously used in calibrating the whole system, because the phase shift between the heat flux and the temperature signal is exactly $\pi/4$.

But what about the transition process, which complicates the measurements even on thin plates? In real cases, where the temperature response oscillates around a non-zero mean value, the impact of the transition process and the influence of the heat accumulation in the semi-infinite body can be assessed by a numerical simulation of the temperature field. This was performed by the **pdepe** function in MATLAB® again. Figure 8 shows the temperature dependency of a semi-infinite body heated by the heat flux oscillating around a non-zero mean value.

The figure also shows the steady periodic solution oscillating around a non-zero mean value of the heat flux and the difference between the steady periodic solution and the numerical solution. It is clear that the difference does not approach zero so quickly as with a plate of finite width.

Carslaw and Jaeger [1] also described the solution of the temperature field in a semi-infinite body heated by the constant heat flux on the surface (page 75) and for zero

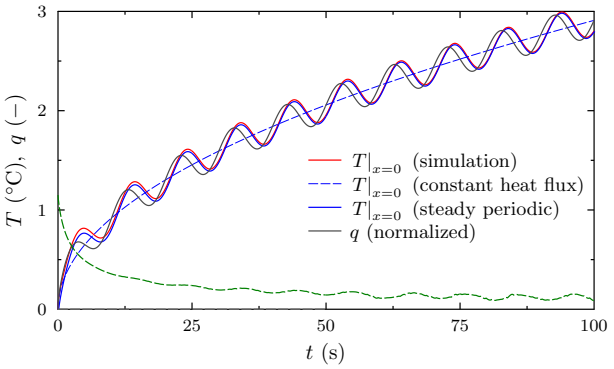

Fig. 8. Temperature response on the surface of a semi-infinite body made from stainless steel. The amplitude of the temperature oscillations is 1000 W m^{-2}, and the mean value is 2000 W m^{-2}. The heat transfer coefficient at the interface is zero. The red line represents the numerical simulation, in comparison with the steady periodic oscillations (blue). The green line slowly approaching a zero value represents the difference between them, magnified by a factor of 10. The gray line represents the heat flux oscillating around the constant mean value.

initial temperature $T_0 = 0$.

$$T = \frac{2\bar{q}}{\lambda}\left\{\sqrt{\frac{at}{\pi}}\mathrm{e}^{-\frac{x^2}{4at}} - \frac{x}{2}\mathrm{erfc}\frac{x}{\sqrt{4at}}\right\} \tag{18}$$

which can be used simply to express the dependency of the surface temperature

$$T|_{x=0} = \frac{2\bar{q}}{\lambda}\sqrt{\frac{a\,t}{\pi}}\,. \tag{19}$$

Carslaw and Jaeger [1] also described the solution for the case of oscillating heat flux $q|_{x=0} = \sin\omega t$ on the surface (page 76)

$$T = \frac{1}{\lambda\sqrt{\frac{\omega}{a}}}\mathrm{e}^{-x\sqrt{\frac{\omega}{2a}}}\sin\left(\omega t - x\sqrt{\frac{\omega}{2a}} - \frac{\pi}{4}\right) + \\ + \frac{2a}{\pi\lambda}\int_0^\infty \frac{\omega\cos ux}{\omega^2 + a^2u^4}\mathrm{e}^{-au^2t}\mathrm{d}u\,. \tag{20}$$

The last term in this equation, when compared to the steady periodic solution on the surface of a semi-infinite body, describes the impact of the transition process caused by the oscillating heat flux at the beginning.

We performed a numerical simulation of the heat transfer in a semi-infinite body, see Figure 8, and the phase shift evaluated by the algorithm was 48.61°. This is close to the theoretical value of 45°, but due to the impact of its deviation on the accuracy of the heat transfer coefficient, a value of 48.61° is unacceptable.

The last question concerns the practical realization of the semi-infinite body. In practice, we would like to use a finite body that would provide results not too different from the results for the semi-infinite body. What should the width of such a body be? Using the dimensionless coordinate $\eta = x/\sqrt{4at}$, we can transform solution (18) to

$$T = \bar{q}\frac{\sqrt{4at}}{\lambda}\left\{\sqrt{\frac{1}{\pi}}\mathrm{e}^{-\eta^2} - \eta\,\mathrm{erfc}\,\eta\right\}\,. \tag{21}$$

Let us find a value of dimensionless coordinate η such that, for the given time, the value of the term in brackets (containing real coordinate x) was equal to, for example, 0.01, 0.005 or 0.001 of the value on the surface ($\eta = 0$ for $x = 0$, and the term is $1/\sqrt{\pi}$). For the chosen values, we get $\eta_{0.01} = 1.6056$, $\eta_{0.005} = 1.7688$ and $\eta_{0.001} = 2.1127$. The temperature field is practically unaffected (0.1 %) at time 100 s at a distance of 82.8 mm for a stainless steel, and 24.4 mm for glass. This value does not reflect the penetration depth of the oscillating solution, However, looking at the damping term in (15) and evaluating its value for stainless steel, for example, criterion 0.1 %, with the same time and frequency of the oscillating heat flux 0.1 Hz, we get $\exp\left(-x\sqrt{\omega/2a}\right) = \exp\left(-\eta\sqrt{2\omega t}\right) = \exp(-2.1127\sqrt{4\,\pi\,0.1\cdot 100} \sim 10^{-11}$. We can see that the impact of the penetration depth is much smaller with an oscillating heat flux than with a constant heat flux.

6 Gnielinski

Heat transfer coefficients were measured on the surface of a horizontal pipe with inner diameter $d = 32$ mm and wall width $\delta = 1.5$ mm. A pipe with length $L = 2000$ mm was made of stainless steel (see Table 1 of the corresponding thermophysical properties). The pipe section 200 mm in length at a distance of 1700 mm from the pipe inlet was irradiated by the heat oscillations generated by two 500 W halogen lamps.

Water at a temperature of 25.16 °C ± 0.2 °C and with a flow rate of 27.37 l min^{-1} ran in the pipe from a closed hydraulic circuit. The thermophysical properties of water at this temperature [13] are: density $\varrho = 997.0$ kg m^{-3}, specific heat capacity $c_p = 4179.2$ J kg^{-1} K^{-1}, thermal conductivity $\lambda_\mathrm{f} = 0.6114$ W m^{-1} K^{-1}, and kinematic viscosity 8.8998×10^{-7} m^2 s^{-1}.

The corresponding Reynolds number (based on a mean volumetric velocity of 0.5672 m s^{-1}) is 20394 in this case, so we are in the region of fully developed turbulent flow [12], i.e. in the region described by Gnielinski's correlation (1). Using this correlation in the calculation of the Nusselt number, without the Hausen correction for now, we get $\mathrm{Nu_m} = \alpha_\mathrm{m}\,d/\lambda_\mathrm{f} = 147.97$ and the corresponding mean heat transfer coefficient $\alpha_\mathrm{m} = 2827$ W m^{-2} K^{-1}.

The turbulent flow in this geometry was modeled using ANSYS® CFD® software. A structured mesh with 40000 elements and the ANSYS® Fluent™ solver were used. Rotational symmetry and the RANS approach (Reynolds Averaged Navier-Stokes), along with the $k-\omega$ SST (Shear Stress Transport) turbulence model were used in the solution of the momentum and energy transport equations. The SIMPLE algorithm for pressure-velocity coupling and second order spatial discretizations for all quantities were used. Iterations were performed until the residuals fell below 10^{-10}. A constant velocity profile was specified at the pipe inlet. A stable turbulent velocity profile developed in the pipe (entrance length 1700 mm). The inlet temperature was 300 K, and the wall temperature of the measuring section 200 mm in length was set to 400 K. The constant thermophysical properties mentioned above were assumed. For the evaluation of the heat transfer coefficient on the inner surface, the reference temperature corresponding to the arithmetic mean of the mixed cup temperatures at the inlet and the outlet of the measuring section was evaluated as $(300.035 + 302.639)/2 = 301.337$ K. The maximum dimensionless size of the mesh element at the pipe wall was $Y^+ = 0.152$.

Table 4 compares the results of our numerical simulation with values based on the Gnielinski correlation. Figure 9 compares local values of the heat transfer coefficients along the measurement section based on Eq. (3) with values obtained in the numerical simulation. It is clear that the mean value based on the numerical simulation is approximately 10 % lower than the Gnielinski correlation (the accuracy can be expected to be 6 – 10 %). The dependency of the local values shows that this difference is mainly affected by the increase in heat transfer at the beginning of the measurement section. After the thermal boundary layer is developed, this difference is much

Table 4. A comparison between the results based on numerical simulations and the analytical results based on engineering correlations. The pressure drop can be expressed from the Darcy-Weisbach equation $\Delta p = \xi \cdot L/d \cdot \varrho\, \bar{u}^2/2$, and the wall shear stress from $\tau_w = \Delta p\, d/4L$.

Quantity	Analytical	Numerical	
Δp	25.602	26.982	Pa
ξ	0.0255	0.0269	
τ_w	1.0241	1.0789	Pa
α_m	3660	3300	$\mathrm{W\,m^{-2}\,K^{-1}}$

smaller. Figure 9 illustrates that the substantial increase in the heat transfer in the development of the thermal boundary layer must be taken into account when using any experimental method focused on local values. We should therefore take into account the location where the measurement is made, and also the way in which the heat transfer surface is heated.

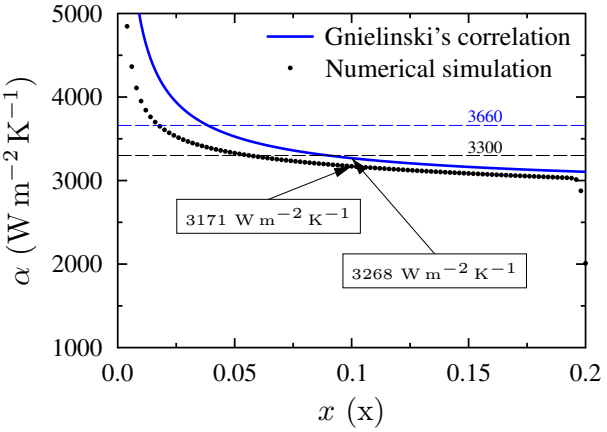

Fig. 9. A comparison of local values of the heat transfer coefficients along the measurement section. Blue color corresponds to (3), black color represents values based on the numerical simulation.

Using the numerical model, we can solve the case of measuring the heat transfer coefficient using the TOIRT method. Because the TOIRT method is a transient method, we have to solve the time dependency of the temperature field and monitor the temperature on the surface of the measuring section. The temperature oscillations are generated by the oscillating heat flux on the surface of the measurement section. The following user-defined function (UDF) was used in the ANSYS® Fluent™ solver as the corresponding boundary condition.

```
DEFINE_PROFILE(hf_t_alpha, thread, position)
{
  real flow_time = RP_Get_Real("flow-time");
  real wTemp, q, q_ave, q_ampl, omega, freq,
  face_t f; real alpha_delta, T_amb;

  freq = 0.1; omega = 2*PI*freq;
  alpha_delta = 3; T_amb = 300;  q_ampl = 2000;
  q_ave = 2*q_ampl;
  begin_f_loop(f, thread)
  {
     wTemp = F_T(f,thread);
     q = q_ave + q_ampl*sin(omega*flow_time)
         + alpha_delta*(T_amb-wTemp);
     F_PROFILE(f, thread, position) = q;
  }
  end_f_loop(f, thread)
}
```

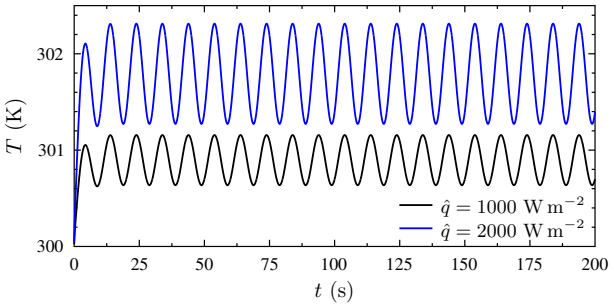

Fig. 10. Time dependency of the surface temperature at a distance of 100 mm from the beginning of the measuring section for two cases of heat flux amplitudes $\hat{q}$ and the heat transfer coefficient between the pipe surface and surroundings 3 $\mathrm{W\,m^{-2}\,K^{-1}}$.

The mean value of the oscillating heat flux was set equal to twice the amplitude of the heat flux, as is done in real measurements. The amplitude was set in such a way that the resulting temperature response amplitude was 0.5 °C, again corresponding to real measurements. Figure 10 shows the time dependency of the surface temperature obtained in the numerical simulation of the heat transfer in the middle of the measurement section.

Processing these data using the algorithm for eliminating the non-oscillating component, we can get the phase shift and the corresponding value of the heat transfer coefficient based on the theoretical Wandelt-Roetzel solution. Assuming zero heat transfer coefficient on the irradiated side ($\alpha_\delta = 0$), the resulting phase shift is 49.575° (ignoring the first period of the temperature response, and if the first period is included, the phase shift is 52.085°). For the heat transfer coefficient on the irradiated side α_δ = 3 $\mathrm{W\,m^{-2}\,K^{-1}}$, the phase shift is 49.541° (52.048° if the first period is included). Both results are for amplitude of the heat flux oscillations 2000 $\mathrm{W\,m^{-2}}$ and time 100 s. The corresponding heat transfer coefficient values, based on the Wandelt-Roetzel solution, are 2844 $\mathrm{W\,m^{-2}\,K^{-1}}$ in both cases. The local heat transfer coefficient value evaluated in the numerical simulation is 3171 $\mathrm{W\,m^{-2}\,K^{-1}}$, see Figure 9, which is 10 % higher than the Wandelt-Roetzel solution. Gnielinski's correlation (3) predicts a value of 3268 $\mathrm{W\,m^{-2}\,K^{-1}}$ at the monitored point.

Let us recall that the evaluation of the experimental data depicted in Figure 5, which represent the same geometry as in the numerical simulations, resulted in a phase shift of 56.322°. The corresponding heat transfer coefficient is then 2101 $\mathrm{W\,m^{-2}\,K^{-1}}$. This value is not correct, because it does not take into account the time constant of the whole measuring system, which was discussed in section 5. If we want to fit the phase shift to the known heat transfer coefficient value of 3268 $\mathrm{W\,m^{-2}\,K^{-1}}$, based on Gnielinski's correlation (3), we will have to determine

a value of 46.253°. We can see that the real phase shift is greater by 56.322 − 46.253 = 10.069°, and this value corresponds to the time constant 10.069/360 × 10000 = 279.7 ms for a period of 10 s, i.e. for 0.1 Hz frequency of the temperature oscillations.

We performed repeated measurements of the heat transfer coefficients along the whole measuring section as a calibration experiment. Using these measurements, we employed a non-linear regression technique to find the time constant of 254 ms, which corresponds to the mean value, according to Gnielinski (see Table 4), or 185 ms for the numerical solution.

7 Conclusions

We have presented some aspects of the TOIRT experimental methods in this paper. It is obvious that further investigations are needed, but we can summarize the following findings.

The measured phase shift should be in the range between 20 and 70° when using the TOIRT method for heat transfer measurements on the surface of a stainless steel plate up to 1.5 mm in width and with 0.1 Hz frequency of the oscillating heat flux. We can expect a relative measurement error of around 10 % for a sufficient large heat flux, creating temperature oscillations with amplitude of 1 °C.

The time constant of the transient process corresponds to $\sim \delta\lambda/(a\alpha)$ for the standard application of the method ($\sim$ 1 mm, $\sim$ 1000 $\mathrm{W\,m^{-2}\,K^{-1}}$, $\sim$ 10 $\mathrm{W\,m^{-1}\,K^{-1}}$). The corresponding time of the transient process is at least 5 times longer.

A numerical analysis of the algorithm for eliminating the non-oscillating component of the measured temperature response showed that its error increases with decreasing amplitudes of the temperature oscillations, and with an increased noise-signal ratio and increased deformation of the signal. To reduce the corresponding error, temperature oscillations with an amplitude of 1 °C or larger are recommended.

When testing the algorithm for eliminating the non-oscillating component for the case of a semi-infinite body, a phase shift of 48.61° was determined, whereas the theoretical value is 45°.

The local heat transfer coefficient in a pipe with turbulent flow was monitored in the middle of a heated section. The corresponding value based on Gnielinski's correlation is 3268 $\mathrm{W\,m^{-2}\,K^{-1}}$, and the value based the numerical simulation is 3171 $\mathrm{W\,m^{-2}\,K^{-1}}$. The value based on applying the Wandelt-Roetzel method to the numerical simulation results is 2844 $\mathrm{W\,m^{-2}\,K^{-1}}$. Is the neglected lateral heat conduction the main reason for this difference, or are there some other reasons (the type of boundary condition, insufficient accuracy of the numerical solution, etc.)?

A comparison was made between the numerical simulation results, the engineering correlations and the experimental data for the case of turbulent flow in the pipe. A phase shift of 254 or 185 ms corresponding to the time constant of the whole measurement process was evaluated, depending on the "correct" mean value that was used for the heat transfer coefficient (Gnielinski's correlation or the numerical solution). Let us recall that a phase shift of one degree at a frequency of 0.1 Hz corresponds to a time delay of 30 ms with a 10 % relative error of the method.

It is clear that further investigations are necessary, especially into various transformation algorithms, the impact of the lateral heat conduction, and the application of the TOIRT method to the laminar flow of liquids. It is obvious that the algorithm for eliminating the non-oscillating component of the temperature response has a large impact on the accuracy of the results. It is necessary to devise a better test, using polynomials of higher orders, using the theoretical solution, etc. The dynamic behavior of the whole measurement system also has a huge impact on the measurement results. There are a various potential approaches. Our future research will involve directly monitoring the light generated by halogen lamps, instead of the calibration experiments mentioned here. The light intensity can then be used for directly controlling the heat flux, or as an input parameter for the TOIRT mathematical model that accounts for the general time dependency of the heat flux.

This work was supported by the Ministry of Education, Youth and Sports of the Czech Republic under OP RDE grant number CZ.02.1.01/0.0/0.0/16_019/0000753 "Research centre for low-carbon energy technologies". Authors also acknowledge support from the Grant Agency of the Czech Technical University in Prague, grant number SGS18/129/OHK2/2T/12.

Finally, the authors express their thanks to Robin Healey, from the Czech Technical University in Prague, for his huge efforts to convert our "English text" into an English text that can be offered to our readers.

Nomenclature

a	thermal diffusivity, $a = \lambda/\rho c_\mathrm{P}$ ($\mathrm{m^2\,s^{-1}}$)
a, b	general parameters (°C, K)
A	amplitude of temperature oscillations (°C, K)
c_p	specific heat capacity ($\mathrm{J\,kg^{-1}\,K^{-1}}$)
d	diameter (m)
f	frequency (Hz, $\mathrm{s^{-1}}$)
f_S	sampling frequency (Hz, $\mathrm{s^{-1}}$)
Gz	Graetz number, $\mathrm{Gz} = \mathrm{Re\,Pr}\,d/L$ (−)
$\mathrm{Gz_x}$	local Graetz number, $\mathrm{Gz} = \mathrm{Re\,Pr}\,d/x$ (−)
L	length (m)
M	mass (kg)
N	number of experimental points (−)
Nu	Nusselt number, $\mathrm{Nu} = \alpha d/\lambda_\mathrm{f}$ (−)
$\mathrm{Nu_m}$	mean Nusselt number (−)
$\mathrm{Nu_x}$	local Nusselt number (−)
Pr	Prandtl number (−)
q	heat flux ($\mathrm{W\,m^{-2}}$)
$\bar{q}$	mean value of heat flux ($\mathrm{W\,m^{-2}}$)
$\hat{q}$	amplitude of oscillating heat flux ($\mathrm{W\,m^{-2}}$)
Re	Reynolds number, $\mathrm{Re} = \bar{u}d/\nu$ (−)
S	surface, heat transfer surface ($\mathrm{m^2}$)
t	time (s)
t_i	time (s)
T	temperature (°C, K)
T_i	measured temperature at time t_i (°C, K)

T_0	initial temperature (°C, K)
T_{eq}	equilibrium fluid (liquid) temperature (°C, K)
T_f	fluid (liquid) temperature (°C, K)
$\bar{u}$	mean velocity ($m\,s^{-1}$)
x, y, z	spatial coordinates of the Cartesian coordinate system (m)
Y^+	dimensionless distance from the wall, dimensionless wall spacing (−)
α	heat transfer coefficient (at $x = 0$) ($W\,m^{-2}\,K^{-1}$)
α_δ	heat transfer coefficient at $x = \delta$ ($W\,m^{-2}K^{-1}$)
β	phase shift (excitation) (−)
δ	width of impinged plate (m)
Δt	time difference, time step (s)
η	dimensionless coordinate, $\eta = x/\sqrt{4at}$ (−)
σ	standard deviation (°C, K)
λ	thermal conductivity, wall thermal conductivity ($W\,m^{-1}\,K^{-1}$)
λ_f	fluid thermal conductivity ($W\,m^{-1}\,K^{-1}$)
ν	kinematic viscosity ($m^2\,s^{-1}$)
ξ	Darcy-Weisbach friction factor (−)
ρ	density ($kg\,m^{-3}$)
τ	time constant (s)
τ_W	wall shear stress (Pa)
φ	phase shift (response) (−)
ω	angular frequency of oscillating heat flux, $\omega = 2\pi f$ (s^{-1})

References

1. H. Carslaw, J. Jaeger, eds., *Conduction of Heat in Solids* (Oxford Univesrity Press, London, 1959)
2. H. Hausen, *Heat Transfer: In Counterflow, Parallel Flow and Cross Flow* (McGraw-Hill, 1983), https://ia801303.us.archive.org/26/items/in.ernet.dli.2015.133989/2015.133989.Heat-Transfer-In-Counterflow-Parallel-Flow-And-Cross-Flow.pdf
3. W. Roetzel, Chem. Eng. Technol. **12**, 379 (1989)
4. W. Roetzel, S.K. Das, X. Luo, Int. J. Heat Mass Transfer **37**, 325 (1994)
5. W. Roetzel, X. Luo, Rev Gén Therm **37**, 277 (1998)
6. P. Leblay, J. Henry, D. Caron, D. Leducq, A. Bontemps, L. Fournaison, *Infrared Thermography applied to measurement of Heat transfer coefficient of water in a pipe heated by Joule effect*, in *QIRT - 11th Quantitative InfraRed Thermography* (2012), pp. 1–10
7. W. Roetzel, S. Prinzen, M. Wandelt, Chem. Eng. Technol. **16**, 89 (1993)
8. M. Wandelt, W. Roetzel, *Lockin thermography as a measurement technique in heat transfer*, in *QIRT 96 - Eurotherm Series 50* (1997), pp. 189–194
9. S. Freund, S. Kabelac, *Measurement of local convective heat transfer coefficients with temperature oscilation IR thermography and radiant heating*, in *Proceedings of HT2005, 2005 ASME Summer Heat Transfer Conference* (2005), pp. 1–7
10. S. Freund, Ph.D. thesis, Der Fakultät für Maschinenbau der Helmut-Schmidt-Universität / Universität der Bundeswehr Hamburg (2007)
11. S. Freund, S. Kabelac, Int. J. Heat Mass Transfer **53**, 3764 (2010)
12. P. Stephan, ed., *VDI Heat Atlas* (Springer, Berlin, Heidelberg, 2010)
13. J. Šesták, J. Bukovský, M. Houška, *Heat processes. Transport a thermodynamic data. (in Czech)* (Publishing Czech Technical University in Prague, Prague, 1996)
14. S. Solnař, Master's thesis, Czech Technical University in Prague (2016)

Appendix

A numerical solution of the heat conduction equation with the given boundary and initial conditions with the **pdepe** function in MATLAB® was made [https://www.mathworks.com]. The function solves an initial-boundary value problem of the parabolic partial differential equation with one independent spatial coordinate. The detailed usage of this function can be found at https://www.mathworks.com/help/matlab/ref/pdepe.html, and our shortly commented source code is presented below.

```
function youcantryme()
% Global variables (parameters)
global OMEGA A LAMBDA ALPHA ALPHAD QAVE QAMPL QFI

% Given parameters
OMEGA = 2*pi()*0.1;
LAMBDA = 15.2; A = 15.2/(7900*501);
ALPHA = 1000; ALPHAD = 3;
QAVE = 2000; QAMPL = 1000; QFI = 0;

t = linspace(0,100,2000); % Time space

% Plate thickness and spatial distribution
DELTA = 0.001; x = linspace(0,DELTA,100);

% PDE solution (0 means Cartesian coordinate system = slab)
[sol] = pdepe(0,@pdefun,@icfun,@bcfun,x,t);

% Results presentation
figure(1); surf(x,t,sol);

end % End of main script

%  PDE, IC and BC definitions
function [c,f,s] = pdefun(x,t,u,dudx) % PDE function
global A % Thermal diffusivity
c = 1/A; f = dudx; s = 0;
end

function u = icfun(x)  % Initial condition
u = 0;
end

function [pl,ql,pr,qr] = bcfun(xl,ul,xr,ur,t)  % BC
global OMEGA A LAMBDA ALPHA ALPHAD QAVE QAMPL QFI
pl = ALPHA*ul; ql = - LAMBDA;
pr = - ALPHAD*ur + QAVE + QAMPL*sin(OMEGA*t + QFI);
qr = - LAMBDA;
end
```